Manuscript Details

Manuscript number	YBENG_2019_479
Title	Comparing different processing methods in apple slices drying. Part 1. Performances of microwave, hot air and hybrid methods at constant temperatures
Article type	Research Paper

Abstract

Hot-air, microwave and hybrid hot air-microwave drying processes for apples slices were realized. Each drying method was carried on operating under a fixed temperature level. To this purpose, a suitable temperature control system based on infrared thermography readout was made. In order to fix slices' temperature, hybrid mode operations required a progressive decrease of MW delivered power meanwhile their temperature approached air temperature. Thus, no preventive strategies were required in order to set up the hybrid mode as elsewhere reported. Drying kinetics were analyzed introducing a new semi-empirical model, which was able to recover the drying behaviour both in terms of weight loss and drying rates. Results showed that the hybrid-drying mode, due to reduced microwave power output, led to a lower drying rate with respect to microwave mode alone. On the other hand, the hybrid method has guaranteed a good quality level of fruit colour comparable to that obtained by microwave and in any case significantly better than slices of apples treated with convection heating. No meaningful differences among drying modes were detected with regard to energy consumptions.

Keywords	Apple; Microwave; Infrared Thermography; Combined Heating; Color
Manuscript region of origin	Europe

Corresponding Author	luciano cinquanta
Corresponding Author's Institution	University of Palermo
Order of Authors	gennaro cuccurullo, Antonio Metallo, Onofrio Corona, luciano cinquanta
Suggested reviewers	Seyed Ahmad Mireei, FERRUH ERDOGDU, Susana Simal

Submission Files Included in this PDF

File Name [File Type]

cover letterBE_1.docx [Cover Letter]

Highlights.docx [Highlights]

MW_Apple_BE.docx [Manuscript File]

Figure 1 Schematic diagram of the microwave lab plant drying system.docx [Figure]

Figure 2 the calibration mapp.doc [Figure]

Figure 3 IR image for MW drying at 65 °C (cold surroundings).docx [Figure]

Figure 4 IR image for hybrid drying (hot surroundings).docx [Figure]

Figure 5a Moisture content curve during hot air heating.docx [Figure]

Figure 5b Drying rate curve during hot-air heating.docx [Figure]

Figure 6 Tslices and Tair during hot air heating at 65°C.docx [Figure]

Figure 7a Maximum instantaneous temp.docx [Figure]

Figure 7b Maximum instantaneous during MW_FA.docx [Figure]

Figure 8a Moisture content [kgwkg d.b.] during MW heating.docx [Figure]

Figure 8b Drying rate curve [kgwkg d.b. min.] during MW heating.docx [Figure]

Figure 9a Moisture content during MW heating.docx [Figure]

Figure 9b Drying rate curve during MW heating.docx [Figure]

Figure 10a Duty_cycles during MWAR drying.docx [Figure]

Figure 10b Energy density rate generation.docx [Figure]

Figure 11 Air and minimum slices' temperatures.docx [Figure]

Figure 12.docx [Figure]

Figure 13a Drying curves for MWFA, HA and HY modes at 65°C.docx [Figure]

Figure 13b Drying rate curves for MWFA, HA and HY modes at 65°C .docx [Figure]

Figure 14 Colour changes (CIElab values).docx [Figure]

To view all the submission files, including those not included in the PDF, click on the manuscript title on your EVISE Homepage, then click 'Download zip file'.

May, 7, 2019

Dear Editor-in-Chief

Dr. W. Day

We submit the original manuscript:

"***Comparing different processing methods in apple slices drying. Part 1. Performances of microwave, hot air and hybrid methods at constant temperatures*** ".

Authors: *Gennaro Cuccurullo, Antonio Metallo, Onofrio Corona, Luciano Cinquanta,*

for publication in "Biosystems Engineering" as original research paper.

Hot air, microwave and combined (HA+MW) drying processes have been carried out on slices of apples, operating at a fixed temperature, using a control system based on infrared thermographic reading. The drying kinetics were analysed and discussed, introducing a new semi-empirical model. In this note 1 only the colour has been evaluated as a qualitative parameter. In note 2, which will follow this one, the effect of the above mentioned heating methods has been evaluated on the ^{1}H-NMR relaxation properties, shrinkage and volatile compounds of apples slices.

We hope this paper is of sufficient interest and is worth of publication in "Biosystems Engineering"

The undesigned, prof. Luciano Cinquanta, attests that:

- the corresponding author and all of the authors have read and approved the final submitted manuscript;
- all the authors have contributed significantly and are in agreement with the content of the manuscript
- no portion of the work has been or is currently under consideration for publication elsewhere
- no portion of the manuscript, other than the abstract, has been previously published or posted in the Internet

Yours sincerely,

Prof. Luciano Cinquanta

***Corresponding author:** Luciano Cinquanta. *Dipartimento di Scienze Agrarie, Alimentari e Forestali, University of Palermo, Italy.*

E-mail: Luciano Cinquanta: Luciano.cinquant@unipa.it

Highlights

- Hot-air, microwave and hybrid drying processes for apples slices were realized
- A temperature control system based on infrared thermography has been developed
- Drying kinetics were analyzed by a model considering weight loss and drying rates
- The hybrid-drying mode led to a lower drying rate with respect to microwave one
- Microwave and hybrid drying have ensured a better color of the apples than hot air

Comparing different processing methods in apple slices drying. Part 1. Performances of microwave, hot air and hybrid methods at constant temperatures

G. Cuccurullo[a], *A. Metallo*[a], *O. Corona*[b], *L. Cinquanta*[b*]

[a] Dipartimento di Ingegneria Industriale, University of Salerno, Italy
[b] Dipartimento Di Scienze Agrarie, Alimentari e Forestali, University of Palermo

Abstract

Hot-air, microwave and hybrid hot air-microwave drying processes for apples slices were realized. Each drying method was carried on operating under a fixed temperature level. To this purpose, a suitable temperature control system based on infrared thermography readout was made. In order to fix slices' temperature, hybrid mode operations required a progressive decrease of MW delivered power meanwhile their temperature approached air temperature. Thus, no preventive strategies were required in order to set up the hybrid mode as elsewhere reported. Drying kinetics were analyzed introducing a new semi-empirical model, which was able to recover the drying behaviour both in terms of weight loss and drying rates. Results showed that the hybrid-drying mode, due to reduced microwave power output, led to a lower drying rate with respect to microwave mode alone. On the other hand, the hybrid method has guaranteed a good quality level of fruit colour comparable to that obtained by microwave and in any case significantly better than slices of apples treated with convection heating. No meaningful differences among drying modes were detected with regard to energy consumptions.

*corresponding author: Luciano Cinquanta; e-mail: luciano.cinquanta@gmail.com

Keywords: Apple, Microwave, Infrared Thermography, Combined Heating, Color

1. Introduction

In microwave assisted drying, heat is not transferred from surface, but it is generated in the bulk of the material by absorption of electromagnetic energy. Typically, the process turns in higher core temperature. Therefore, internal water is pushed outwards creating a porous structure that promotes water flow from the interior to the surface of the material thus enabling fast drying, (Drouzas, Tsami & Saravacos 1999). Despite that, MW driven process can lead to high non-uniform temperature distribution inside the samples as the result of high uneven electromagnetic field in the oven. In addition, as moisture is lost during the process, strong energy densities modifications can happen because of both the marked temperature-dependence of the MW absorption process and the decrease in volume of the material. In such conditions, useful nutrients can be pumped out, worsening the quality of the product. In the above framework, researchers have studied various microwave power control profiles, including intermittent and continuous methods each featured by control strategies intended to avoid or limit over-heating due to changing heat generation, (Li, Wang, Raghavan & Cheng 2006; Cuccurullo, Giordano, Metallo & Cinquanta 2018). Measuring temperatures inside a MW oven is not an easy task to perform because of the inability of traditional metallic probes to couple with the electromagnetic field and to high spatial temperature gradients achieved in the applicator load. In light of these considerations, the role of infrared thermography is to be highlighted as a unique way for the creation of a proper temperature control system (Cuccurullo, Giordano, Metallo & Cinquanta 2017). On the contrary, convective drying is more efficient near and on the surface (Alibas, 2007), apart from undesirable hardening effects (Kumar, Millar & Karim 2014). Obviously, convective hot-air drying is preferable due to its simplicity, but two major drawbacks are its low energy efficiency and long drying time (Ashtiani, Sturm & Nasirahmadi 2018). The combination of both drying methods could lead in optimal performances, since reduced temperature gradients inside the samples under test are expected compared to MW drying alone (Albanese, Cinquanta, Cuccurullo & Di Matteo 2013; Zhao, et. al 2014). A proper combination of both operating modes is still an open question (Zhao et al. 2014); two ways of combining MW with hot air are recognized (Schiffmann 1995):

1. applying MW energy at the early stage of the dehydration process. The interior of the sample is quickly heated to evaporation temperature and the vapor is forced outwards allowing hot air to remove water from the surface;
2. applying MW energy at the late stage of the drying process when conventional drying is less efficient. The outward flux of vapour forced by MWs reduces the shrinkage and the subsequent restriction to diffusion, (Maskan, 2000). In some cases, applying microwave drying in the last stage of the dehydration process can also be very efficient in removing bound water from the product. Unlike the above procedures, wishing to exploit all the above-mentioned advantages, the method introduced in the present paper foresees the contextual application of both MW and hot air heating during all the course of the drying operations. Single mode operations, i.e. convective and MW alone, were considered comparatively. In any case, operating by MWs required a continuous adjustment of the delivered power for keeping a fixed thermal level for the apple slices under test. Results are presented and discussed by comparing the single and coupled drying techniques in terms of processing time, energy efficiency and product colour quality.

2. Materials and method

2.1 Drying equipment

Drying experiments were carried out using a Lab scale MW plant (Fig. 1) housing a magnetron with a nominal power output of 3 kW at 2.45 GHz. The reverberating chamber was a metallic cubic room (1m^3), thermally insulated by Isolek EX300LBD panels (thermal conductivity 0.031 W/mK UNI 10351), 20 mm thick. The magnetron delivered power was adjusted continuously by a suitable control system able to fix the slices temperature level to the desired setpoint. To this purpose, sample surface temperatures were detected by computer aided thermography system based on the ThermaCAM Flir P65, installed on the oven top surface; the camera looked inside the reverberating chamber through a square hole (70 mm x 70 mm). The hole was properly shielded with a metallic grid, which allowed IR vision inside the cavity. The IR image encompassed almost the 35% of the total applicator load. A helicoidal fan was employed in order to cool the shielding grid. A PCE-PA600 wattmeter with a precision of 1W and a resolution of ± 1.5% was used to acquire the instantaneous power in use.
A conventional hot-air drying unit was prepared by equipping the oven with an air circulation system alternatively allowing both external and recirculated air to be blown inside the cavity. A centrifugal fan (Leister medium pressure blower silence, rated at 250W) was connected to an inline electric heater (Leister LE5000, 4.5 kW) placed on the inlet pipe. The heater was triggered by a thermocouple placed on the exhaust air pipe in order to obtain a stable air temperature inside the oven. The related air flow was fixed at 20 m^3 h^{-1} with the aid of a glass tube flow meter (Asa, Italy) and distributed inside the cavity through a specifically designed manifold placed on the bottom of the oven, see Figure 1. A turntable, rotating @ 7 rpm, supported the samples to test. It was realized by a teflon annulus (500 mm i.d., 550 mm o.d.) covered with a high-density polyethylene squared grid (10 mm x 10 mm). It was suspended from the top of the oven and connected to a technical balance using nylon wires (Gibertini, EU C1200 max 1200 ± 0.01 g) to measure on-line sample mass. The acquisition rate was of 120 samples per minute. A specifically realized software (7.1 LabView®, National Instruments Corp., Austin, Texas) was employed for both data acquisition/reduction. The code collected the weight loss, the IR data and the exhaust air probe data for controlling purposes (Humidity Temperature Sensor TFG80 Duct version with Polyga® measuring element). In particular, the IR camera delivered samples surface radiosity map each 0.9 s, which allowed recovering the corresponding temperatures as the result of a preliminary calibration accounting for the presence of the grid. At this point, the code extracted a specific temperature from the image, according to the procedure described below,

see paragraph 2.3; based on such temperature reading, the computer program controlled the power supply to the magnetron with a DAQ board (AT MIO 16XE50, National Instruments, Austin, Texas) by means of an ON/OFF strategy.

2.2 Samples preparation

Fresh apples (*Golden delicious*), were purchased from a local market and stored at 4°C before drying. Apples were cut into slices (10±0.2 mm thick, 20±0.3 mm diameter) with a sharp-edged copper pipe. Samples were washed in hot water at 90°C for one minute for blanching treatment, and then placed into cold water at 4°C for a further minute to avoid over processing; finally, the water excess was removed. The average initial moisture content of the blanched samples was about 86.1 ± 0.9% (w.b.) as resulted by heating samples in a convective oven at 105 °C, until a constant mass was achieved. Slices were positioned on the turning table at regularly spaced positions. The initial sample mass was about 200 g.

2.3 Drying modes

Drying equipment was operated according to four different modes:

1) MWAR drying mode, based on microwaves and encompassing continuous air recirculation inside the oven; @ 35, 55 and 65 °C;
2) MWFA drying mode, based on microwaves and encompassing continuous fresh air inlet; @ 35, 55 and 65 °C;
3) HA drying mode, based on convection with hot air; @ 35, 55, 65 and 75 °C;
4) HY drying mode, based on both MW and convection with hot air; @ 65 °C.

All the tests were carried on by fixing temperature level, drying curves; air and IR image sequence of the sample to dry were recorded by a personal computer. Post processing of the IR images allowed retrieving the maximum, minimum and average sample temperatures along the drying process. All experiments were performed in triplicate and the related averages were collected and reported along with standard/absolute error of the mean.

2.4 Data acquisition and reduction

2.4.1 Temperature control for cold surroundings

In order to take into account the presence of the shielding grid through which the camera looked at the target slices, a preliminary calibration was required: the complete procedure is reported in a previous work (Cuccurullo, Giordano, Albanese, Cinquanta & Di Matteo 2012). When MW heating was the only operating mode, air and oven walls were almost at room temperature while the drying process went on. Therefore, the hottest point in the IR image belonged to the apple slices domain. Accordingly, it was easy to setup a control strategy based on the knowledge of the instantaneous maximum temperature retrieved from the image (Fig. 2). The code extracted the maximum temperature from the actual IR image and then compared it to the set point in order to achieve the required on/off strategy. Three fixed levels were considered for the maximum temperature, i.e. 40, 60 and 70 °C. After a suitable post processing of the image sequence, the corresponding average temperatures of the apples were extracted; they turned out to be nominally 35, 55 and 65 °C (see table 1 for the corresponding exact values).

2.4.2 Temperature control for hot surroundings

In addition to MW operations, hybrid and hot air heating modes were realized and an updated calibration was required, since surrounding temperatures were higher than apples temperature. Calibration was performed by detecting slices surface temperatures both by an optical fiber sensor (T_s) and by the IR camera (T_{IR}), for several grid temperatures (T_{grid}). In order to keep grid temperature as low as possible when operating with hot air, a fan was employed as a result, grid temperatures ranged from 30 to 34°C, essentially depending on the temperature set for the air inside the oven. A relationship providing the function $T_s = T_s(T_{IR}, T_{grid})$, (Fig. 3), was then set up by a bi-linear interpolation for the 2-D gridded data (Table 2).

While performing the drying process in presence of hot air, the slices turned out to be colder than the surroundings due to water evaporation (Fig. 4); therefore, the minimum absolute slices temperature was easily detectable by searching for the instantaneous minimum temperature in the image. Then, the control strategy for fixing the temperature level in the oven was based on such parameter. Three levels for minimum temperature were considered; after post processing the image sequence, the corresponding average turned out to be nominally 55°C, 65 and 75°C (Table 1).

2.4.3 Weight loss data

The technical balance weighed about 120 times per minute; each two minutes, the code performed a polynomial regression of the experimental data to smooth out the short-term oscillations due to the turntable unbalance. Then, the corresponding d.b. moisture content and drying rates (DR) were calculated.

$$M_d = (\text{mass of water})/(\text{mass of solid}) = m_w/m_s \qquad (1)$$

Tests ended when a final moisture content of about 20% (w.b.) was achieved, corresponding to a water activity (Aw) < 0.7, values able to ensure microbiological stability of dried fruits. Subsequently, the samples were vacuum-sealed in polyethylene bags and stored at 5±0.5°C for colour quality evaluation. Since the behaviour of a food material during MW or hybrid drying processes is complex, the drying kinetics is usually studied by fitting data into semi empirical models, e.g. Newton, Page, Henderson-Pabis, Weibull, Logarithmic and Midilli–Kucuk (Ashtiani et al., 2018). Fitting involves the dimensionless moisture ratio during the drying process

$$MR(t) = (Mw - Mwe)/(Mw0 - Mwe) \cong Mw/Mwo \qquad (2)$$

where M_{w0}, M_w and M_{we} represented the moisture content w.b. at the initial time, at any given time and at equilibrium, respectively. Here, fitting was performed for the experimental sets of drying-rate data by the following function:

$$\mathrm{DR(t)} = a - b\, t^c \exp(-d\, t^e) \qquad (3)$$

where the five constants *a*-*e* are equation-fitting coefficients, DR is expressed in $kg_w/(kg_{db}\ s^{-1})$ and *t* in minutes (Fig. 5b). In order to state the appropriateness of the above fit, the moisture content on d.b. was coherently obtained by integrating eq. (3):

$$M_d(t) = a\ t + (b/d)\cdot c^{-k}\cdot(\Gamma(k, ct^d) + \Gamma(k,0)) + M_{do} \qquad (4)$$

were $k = (1+e)/d$ and $\Gamma(a, z)$ is the incomplete gamma function.

2.4.4 Colour measurement

The colours of the apple slices, before and after drying, were evaluated using a colorimeter (Chroma Metre CR-400, Minolta, Osaka, Japan) with the measurement of the 3 parameters of the Hunter scale: L indicates the brightness, a* the colour scale on an axis from green (-) to red (+) and b* from blue (-) to yellow (+). The colorimeter was automatically calibrated before each color measurement with a standard white plate having L*, a* and b* values of 97.55; 0.09 and 1.80 respectively. In each measurement, five samples were selected and for each trial, the measurements were repeated four times. In addition, the total color difference (ΔE), white index

(WI), Chroma (C*), and Hue angle (h°) were computed from the L*, a*, b* according to International Commission on Illumination (CIELab).

3. Result and discussion

3.1 Hot air mode

Hot air mode tests were carried on following the procedure outlined before. The d.b. moisture content of apple slices along with the drying time is shown in Figure 5a for selected temperature levels (35, 55, 65 and 75°C). As expected, increasing air temperature, led to reduce drying times of apples with increasing sensibility. The conventional duration of the drying process is evidenced on the plots, whereas quantitative results are reported in Table 3. The corresponding drying rate curves (Fig 5b) roughly exhibit the three periods traditionally featuring processes at constant temperature (Li, Raghavan, Wang & Vigneaultd 2011): - I) heating-up period, in which the temperature of the product increases with time and therefore the material starts to lose moisture at increasing rates; - II) constant drying rate period, after a stable temperature profile is reached and drying rates are highest; - III) falling rate period, in which drying rates progressively slow down due to diffusion controlled mechanism inside the slices. Curves are more peaked with increasing temperature, therefore the extension of the II region progressively vanishes; this behaviour was found elsewhere, e.g. (Ashtiani et al., 2018; Roknul, Zhang, Mujumdar & Wang 2014; Bhattacharya, Srivastav & Mishra 2015). In both figures, the experimental points are compared with the predicted curves according to equations (3) and (4); the corresponding fitting coefficients and the goodness of fit in terms of root mean square error (RMSE) are reported in Table 4. As general rule affecting all the drying conditions, drying rates (DR) curves offer predictions more accurate than the ones featuring the corresponding Md curves. Nevertheless, eq. (4) confirms predictions given by eq. (3) allowing a good fit of experimental data for all the drying technique under consideration.

With regard to temperature trend, the oven air temperature required about ten minutes to reach the set point at 65°C, whereas temperatures of the apple slices progressively increased; they aimed to asymptotically recover the air temperature toward the end of the drying process, when evaporation is negligible, as shown in Figure 6.

3.2 Microwave mode

Microwave drying test were carried on both by recirculating air and by introducing fresh air inside the cavity. Three-selected level, namely 40, 60, 70°C, were set the instantaneous maximum temperature in the IR image. The corresponding average temperatures turned out to be nominally 35, 55, 65°C. The related standard deviations are collected in Table 4. The controlled variable evolution along with the drying time is reported in Figures 7a and 7b. Unlike convective heating, volumetric heat generation due to microwave heating causes a driving gradient from the core of the slice toward the surface thus the mass transfer is enhanced, and drying times are noticeably reduced with respect to the convective mode already examined. The ability of the control system to keep temperature level fixed at the desired values clearly appears. As expected, faster drying occurs with increasing temperatures, which requires increased heat generation inside the samples under test. Of course, drying time decreases in presence of continuous fresh air inlet, which leaves essentially unaffected the related energy consumptions.

It can be further observed that the higher the temperature level, the higher the temperature fluctuations (Cuccurullo et al., 2012; Cuccurullo et al., 2017): the addressed behaviours can be probably due to both enhanced energy densities (Cuccurullo et al., 2018) and to increased cooling speed after switching-off the magnetron. Augmented energy densities should be related to product shrinkage and progressive water content reduction per unit of volume. For the latter reason, toward the end of the process at constant temperature, fluctuations become wider. With reference to the moisture content evolution, the continuous introduction of fresh air (FA) reduced time for drying with respect to air recirculation operations (AR) at the same temperature level (Fig. 8a and 9a). The difference between the two operating modes is stronger as the temperature level increases: a reduction of 31.7% is observed with reference to the lower temperature level, while 44.2% and 50.0% correspond to the middle and higher level, respectively. Curve fitting is quite satisfactory; results are summarized in Table 4. Once again, the corresponding DR curves (Fig. 8b and 9b) show the trend outlined before but here faster mass transfer makes the constant rate period to vanish. This behaviour was reported by several authors (Maskan, 2000; Wang, Xiong & Yu 2004; Swain Samuel, Bal, Kar & Sahoo 2012; Mirzabeigi, Sadeghi & Mireei 2016). The overall energy consumptions were evaluated by processing the ON/OFF sequence of the magnetron power. They turned out to be almost independent of the drying mode in use (Table 1). The duty cycle dimensionless plots (Fig. 10a), related to MWAR operations, show that, for a fixed setpoint temperature, curves resemble the behaviour featuring the drying rate evolution: the delivered power steeply grows until a maximum is attained, after which it exhibits progressively decreasing decays rates; the maximum falls well beyond after the time corresponding to drying rate peek. Power increased with increasing the setpoint temperature for any time. It seems interesting to evidence that the corresponding energy rate densities are monotonically increasing with time (Fig. 10b). Similar behaviour is also retrieved for MWFA mode, where stronger evaporation rates require augmented energy consumptions but shorter time for completing the process. Therefore, tests carried on by MWFA mode exhibit the peek for the delivered power earlier than the ones by AR mode.

3.3 Combined MW-hot air heating

Tests were carried out by keeping the minimum temperature of the apple slices under control, while air temperature was fixed at 65°C (Fig. 11). A preliminary phase of about 8 minutes was necessary, during which the system operated only in convective mode: in this way, the turning table and the walls of the oven warmed up approaching the air temperature. Therefore, the apple slices were colder than the surroundings and the instantaneous minimum temperature of the detected scene decreased within them. In this condition, the minimum apples temperature was obviously chosen as the controlled variable. By processing the sequence of the thermographic images (recorded every 5 minutes), the slices average temperature for each image were evaluated. Then, the average temperature of the slices, evaluated over the whole process duration, was found to be about 4°C higher than the setpoint minimum temperature. Results are summarized in Table 4 where the same parameter related to MWFA tests are reported for comparison. The latter result enabled to suitably tune the set point for the minimum temperature in order to realize both for air and slices the same temperature level, i.e. 65°C.

The required time-to-dry in the HY mode was 122 min, value included between the HA and MW ones at the same reference temperature. In this case, the increase of the external temperature can become a disadvantage, since it increases the time for which magnetron is off and therefore decreases the drying rate, even if it favours evaporation at the interface. On the other hand, the combined heating system reduced the amplitude of temperature fluctuations (Fig.12), because it smoothed out the uneven distribution of temperature due to the MW mode alone. Lastly, the drying kinetics (Fig. 13a) were similar to those described above, but there was an increase in the duration of the final phase (13b).

3.4. Colour changes

The different heat treatments have resulted in small differences in the colour of dried apple slices (Fig. 14). This is probably also due to the blanching pre-treatment, which inactivated the PPOs (polyphenol oxidases) responsible for enzyme browning. Compared to fresh samples, the red index (a*) increased significantly in all dried samples, but less in the sample MW heated at 65 °C. Overall colour variations were minor in samples heated with MW at 65 °C (ΔE=19.8) and at 55° (ΔE=20.7), followed by combined heating at 60 °C (ΔE=21.7). These results indicated the effectiveness of MW and hybrid heating in drying compared to convective system (ΔE=25.0 @ 65°C), in preserving the chromatic characteristics of the samples, mainly because of the shorter heat treatment time.

4. Conclusions

Three different drying modes were compared in order to process apple slices at constant temperatures. A hybrid mode was realized by combining microwaves and hot air drying meanwhile adopting a suitable temperature control based on IR thermography readout. The effect of the latter processing mode was evaluated in terms of drying rate and quality of the final product. Significant differences in terms of drying times were found among the configurations under test. The time required to complete the drying process at 65 °C varied from about 44 min for the MW with fresh air ventilation to 122 min for combined heating and 238 min for the hot air. MW drying times significantly decreased with the addition of air renewal. Accordingly, overall colour variations were minor in samples heated with MW at 65°C (ΔE=19.8).Combined mode showed best performance respect to convective mode but worse than MW. Results also indicated that the overall energy requirements were almost unchanged operating with the different drying modes, yet specific energy generation rates were progressively increasing during the process.

References

Albanese, Cinquanta, Cuccurullo, & Di Matteo, 2013. Effects of microwave and hot-air drying methods on colour, beta-carotene and radical scavenging activity of apricots. *International Journal of Food Science & Technology*, 48, 1327-1333.

Alibas I. (2007). Characteristics of Chard Leaves during Microwave, Convective, and Combined Microwave-Convective Drying. *Drying Technology* 24, 1425-1435.

Ashtiani M. S-H., Sturm B. & Nasirahmadi A. (2018). Effects of hot-air and hybrid hot air-microwave drying kinetics and textural quality of nectarine slices. *Heat and Mass Transfer* 54, 915–927.

Bhattacharya M., Srivastav P.P. & Mishra H.N. (2015). Thin-layer modeling of convective and microwave-convective drying of oyster mushroom *(Pleurotus ostreatus)*. *Journal of Food Science & Technology* 52, 2013–2022.

Cuccurullo G., Giordano L., Albanese D., Cinquanta L. & Di Matteo M. (2012). Infrared thermography assisted control for apples microwave drying. *Journal of Food Engineering*, 112 319–325.

Cuccurullo G., Giordano L, Metallo A. & Cinquanta, L. (2017). Influence of mode stirrer and air renewal on controlled microwave drying of sliced zucchini. *Biosystems engineering,* 158, 95-10

Cuccurullo G., Giordano L., Metallo A. & Cinquanta L. (2018). Drying rate control in microwave assisted processing of sliced apples. *Biosystems engineering* 170, 24-30.

Drouzas A. E., Tsami E. & Saravacos G. D. (1999). Microwave vacuum drying of model fruit gels. *Journal of Food Engineering*, 39, 117–122.

Kumar C., Millar G.J. & Karim M.A. (2014). Effective diffusivity and evaporative cooling in convective drying of food material. *Drying Technology*, 33, 227-237.

Li Z., Wang N., Raghavan G. S. V. & Cheng W. (2006). *A microcontroller-based, feedback power control system for microwave drying processes.* Applied engineering in Agriculture, 22, 309-314.

Li Z., Raghavan G. S. V., Wang N. & Vigneaultd C. (2011). Drying rate control in the middle stage of microwave drying. *Journal of Food Engineering,* 104 234–238.

Maskan M. (2000). Microwave/air and microwave finish drying of banana. *Journal of Food Engineering*, 44, 71–78.

Mirzabeigi Kesbi O., Sadeghi M. & Mireei S.A. (2016). Quality assessment and modeling of microwave-convective drying of lemon slices. *Engineering in Agriculture, Environment and Food,* 9:216–223.

Roknul A.S.M., Zhang M., Mujumdar A.S. & Wang Y. (2014). A comparative study of four drying methods on drying time and quality characteristics of stem lettuce slices *(Lactuca sativa L.)*. *Drying Technology,* 32:657–666.

Schi□mann R. F. (1995). Microwave and dielectric drying. In A. S.Mujumdar (Ed.), *Handbook of industrial drying-1* (345–372) New York: Marcel Dekker Inc.

Swain S, Samuel D.V.K., Bal L.M., Kar A. & Sahoo G.P. (2012). Modeling of microwave assisted drying of osmotically pretreated red sweet pepper *(Capsicum annum L.)*. *Food Science and Biotechnology,* 21:969–978.

Wang J., Xiong Y.S. & Yu Y. (2004). Microwave drying characteristics of potato and the effect of different microwave powers on the dried quality of potato. *European Food Research and Technology,* 5:500-506.

Zhao D., An K., Ding S., Liu L., Xu Z. & Wang Z. (2014). Two-Stage Intermittent Microwave Coupled with Hot-Air Drying of Carrot Slices: Drying Kinetics and Physical Quality. *Food Bioprocess Technology*, 7:2308–2318

Figure captions

1) Schematic diagram of the microwave lab plant drying system.

2) IR image for MW drying at 65 °C (cold surroundings).

3) The calibration map.

4) IR image for hybrid drying (hot surroundings).

5a) Moisture content curve during hot air heating of apple slices at 55, 65 and 75 °C.

5b) Drying rate curve during hot-air heating of apple slices 55, 65 and 75°C.

6) T° of slices and T° of air during hot air heating at 65°C.

7a) Maximum instantaneous temperatures for MW drying with air ricircle.

7b) Maximum instantaneous during MW-FA heating of apple slices corresponding to at 35, 55 and 65 °C average temperatures.

8a) Moisture content [kgwkg d.b.] during MW heating of apple slices with air recirculation at 35, 55 and 65 °C.

8b) Drying rate curve [kgwkg d.b. min.] during MW heating of apple slices with air recirculation at 35, 55 and 65°C.

9a) Moisture content during MW heating of apple slices with continuous fresh air introduction 35, 55 and 65 °C.

9b) Drying rate curve during MW heating of apple slices with continuous fresh air introduction at 35, 55 and 65 °.

10a) Duty_cycles during MWAR drying at 35, 55 and 65 °C.

10b) Energy density rate generation during MWAR drying at 35, 55 and 65 °C.

11) Air and minimum slices' temperatures during hybrid heating.

12) Spatial average slices' temperatures.

13a) Drying curves for MWFA, HA and HY modes at 65°C.

13b) Drying rate curves for MWFA, HA and HY modes at 65°C.

14) Colour changes in dried apples (CIElab values).

Nomenclature

Symbol or abbreviation (Unit)	& Meaning
MW	microwave
IR	infrared
RMSE	root mean square error
d.b	dry basis
i.d	internal diameter
o.d	outside diameter
w	water
Md(t) ( )	moisture content on dry basis
mw(t) (kg)	moisture content at time t
md (kg)	dry mass
DR(t) (s 1)	drying rate
DRmax(s 1)	target value for DR(t)
a (s 1)	equation fitting coefficient
b (s c 1)	equation fitting coefficient
c ( )	equation fitting coefficient
d (s e)	equation fitting coefficient
e ( )	equation fitting coefficient
Tmin [°C]	instantaneous minimum image temperature
Tmax [°C]	instantaneous minimum image temperature
tc (s)	characteristic time for which M_d % 0.15
T_{IR} [° C]	IR thermography temperature readout
a*	red index
b*	yellow index
L*	brightness
PPO	polyphenol oxidase

Table 1 – Microwave tests summary

	MWAR35	MWFA35	MWAR55	MWFA55	MWAR65	MWFA65
average slice temperature [°C]	35.7±1.6	35.1±1.7	53.9±1.8	53.1±2	63.7±2.7	62.5±3.1
maximum slice temperature [°C]	40.8±1.9	40.3±1.9	60.5±2.2	59.8±2.4	70.8±2.6	68.7±2.8
tot.time [min]	202	138	104	58	87.9	44
time_on [min]	26.6	27.4	26	25.6	30	26
time_off[min]	175.4	110.6	78	32.4	57.9	18
time_on/time_off [min]	0.13	0.20	0.25	0.44	0.34	0.59
energy consumption [kWh]	1.33	1.37	1.3	1.28	1.5	1.3

Table 2 Fitting parameters used for calibration function

	T_{grid}[°C]	m	q	Dev.st
T_s = m T_{IR} + q and relative fit quality	30	4.65	134.8	0.329
	32	4.34	125.8	0.330
	34	4.33	129.3	0.332

Table 3 Drying performances

Drying conditions	Drying Time [min]	fitting coefficients					DR[s^{-1}]	Md[ ]
		a	-b	c	d	e		
MWAR35	202 ± 4.3	9.59 10^{-5}	1.13 10^{-3}	6.24 10^{-3}	1.31	1.4 10^{-1}	1.64 10^{-4}	5.07 10^{-3}
MWAR55	138 ± 2.3	1-32 10^{-4}	1.85 10^{-3}	2.56 10^{-2}	1.20	3.4 10^{-1}	3.59 10^{-4}	4.17 10^{-2}
MWAR65	104 ± 3.3	6.78 10^{-5}	7.51 10^{-3}	8.5 10^{-1}	5.4 10^{-1}	9.72 10^{1}	6.89 10^{-4}	9-16 10^{-2}
HA35	716± 2.3	-6.025 10^{-6}	1.7 10^{-4}	8.24 10^{-3}	0.897	2.1 10^{-1}	2.7 10^{-4}	9 10^{-2}
HA55	288 ± 2.4	2.59 10^{-5}	2.1 10^{-4}	2.4 10^{-1}	5.81 10^{-1}	8.96 10^{-1}	6.55 10^{-5}	9 10^{-2}
HA65	238 ± 3.1	-4.03 10^{-6}	2.57 10^{-4}	4.6 10^{-1}	4.93 10^{-1}	0.109 10^{-1}	6.3 10^{-5}	9.1 10^{-2}
HA75	146 ± 2.3	9.2 10^{-5}	-4.1 10^{-4}	3.78 10^{-2}	9.74 10^{-1}	4.3 10^{-3}	1.26 10^{-4}	1.1 10^{-1}
MWFA35	138 ± 3.9	1.98 10^{-4}	-1.1 10^{-3}	1.78 10^{-2}	1.27	4.06 10^{-1}	2.86 10^{-4}	6.7 10^{-2}
MWFA55	58± 2.6	2.69 10^{-4}	-2.31 10^{7}	2.38 10^{1}	1.9 10^{-1}	6.4	7.79 10^{-4}	1.01 10^{-1}
MWFA65	44± 2.4	5.9 10^{-4}	-1.33 10^{-3}	5.96 10^{1}	1.5 10^{-1}	1.11 10^{1}	1.2 10^{-3}	9.7 10^{-2}
HY	122± 3.4	-1.31 10^{-5}	-4.5 10^{-3}	3.04	3 10^{-1}	1.43	6.16 10^{-4}	6.9 10^{-2}

Table 4 Average slice temperature during the drying process

operation mode	MWAR35	MWAR55	MWAR65	HY
controlled variable	Tmax	Tmax	Tmax	Tmin
average temperature for the controlled variable [°C]	40.8±1.96	60.5±2.13	70.8±2.6	60.5±2.6
average slice [°C]	35.7±1.6	54±1.8	63.7±2.7	64.8±1.2

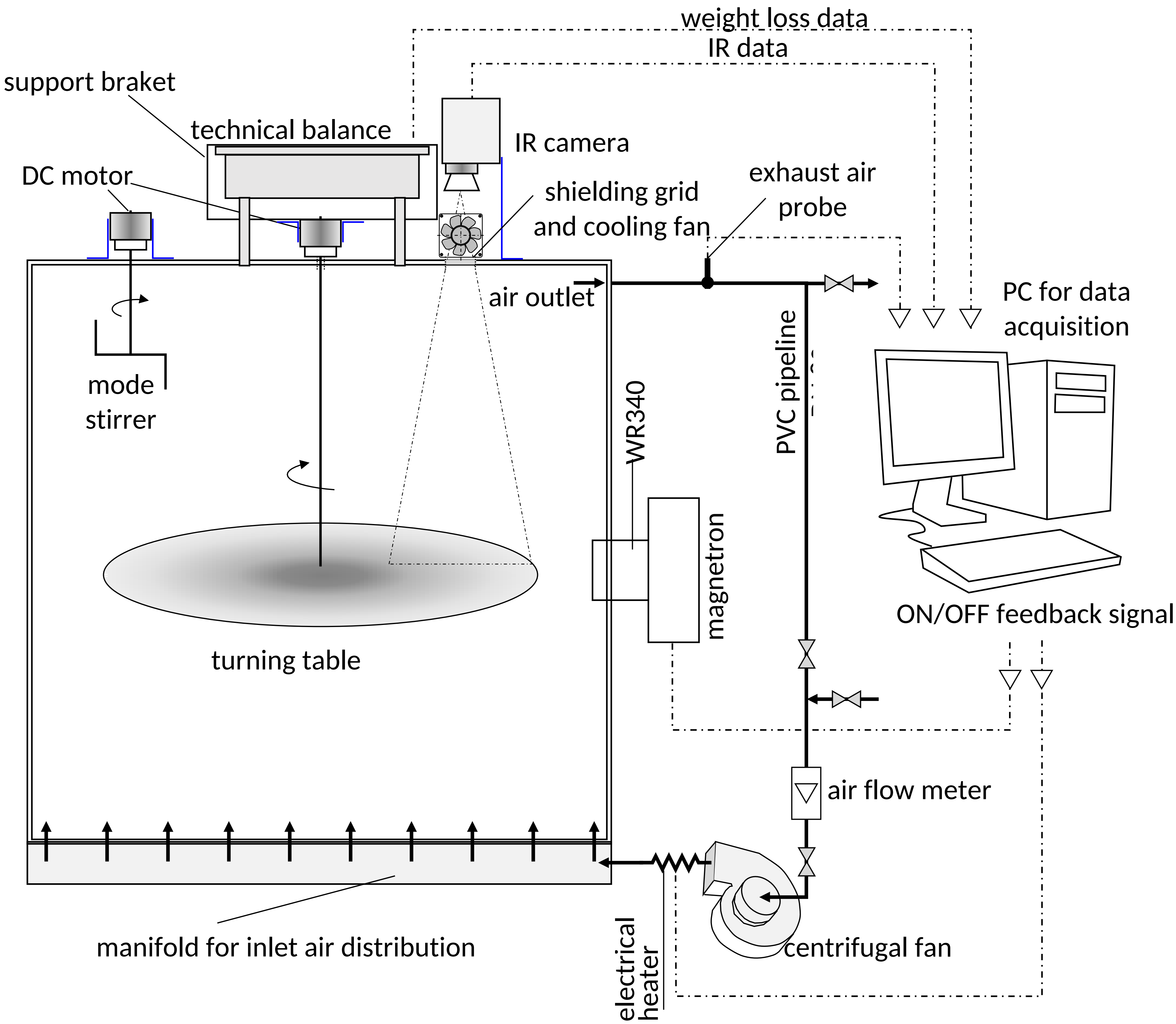
weight loss data
IR data
support braket
technical balance
IR camera
DC motor
shielding grid
and cooling fan
exhaust air
probe
air outlet
PC for data
acquisition
mode
stirrer
WR340
PVC pipeline
magnetron
turning table
ON/OFF feedback signal
air flow meter
manifold for inlet air distribution
electrical
heater
centrifugal fan

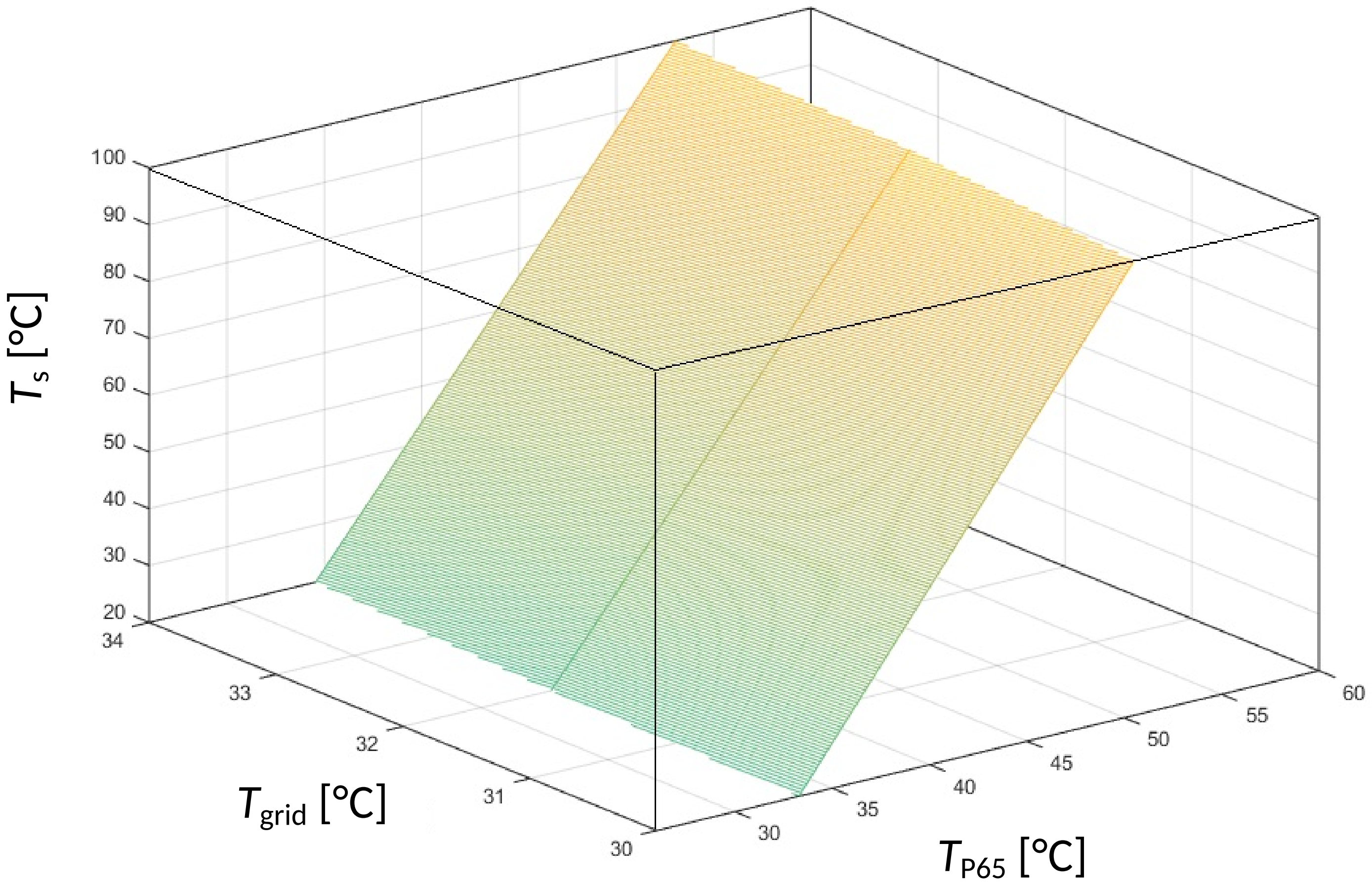

T_s [°C]
100
90
80
70
60
50
40
30
20
34
33
32
31
30
T_{grid} [°C]
30
35
40
45
50
55
60
T_{P65} [°C]

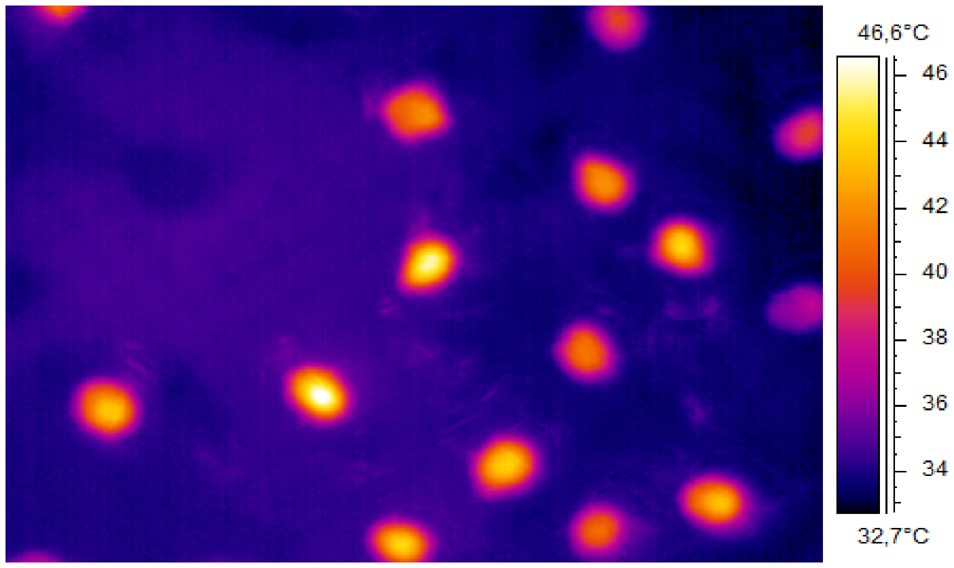
46,6°C
46
44
42
40
38
36
34
32,7°C

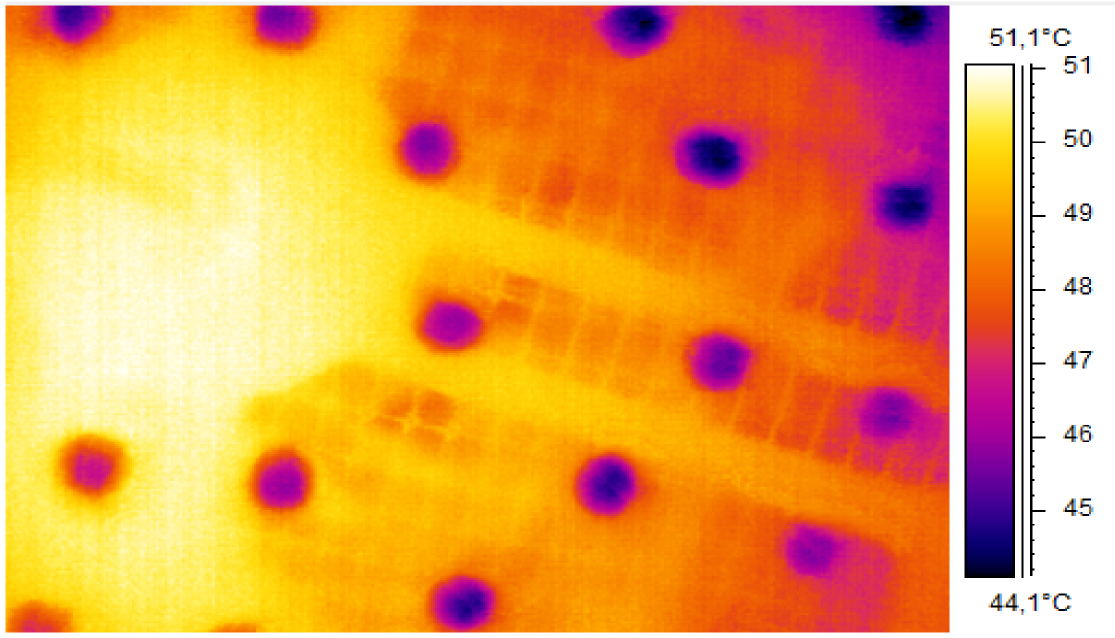
51,1°C
51
50
49
48
47
46
45
44,1°C

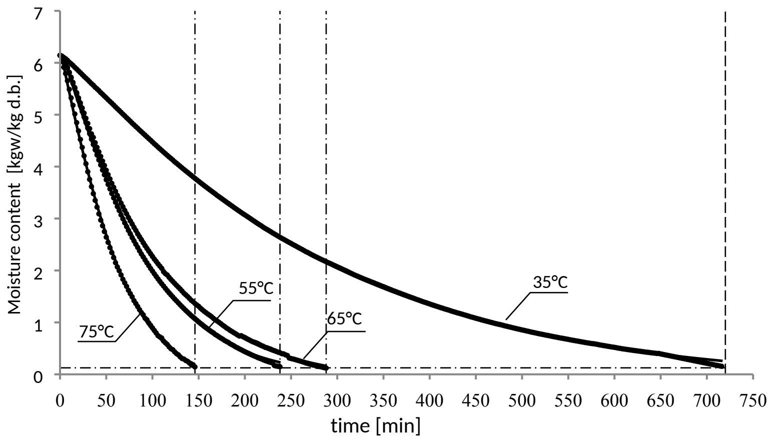

7
6
5
4
3
2
1
0
Moisture content [kgw/kg d.b.]
0
50
100
150
200
250
300
350
400
450
500
550
600
650
700
750
time [min]
75°C
55°C
65°C
35°C

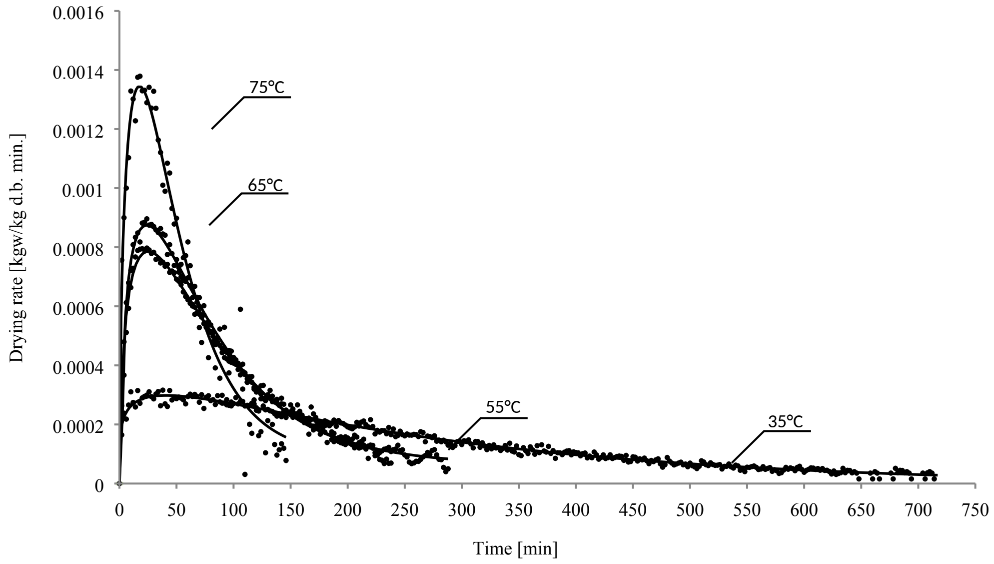
0.0016
0.0014
0.0012
0.001
0.0008
0.0006
0.0004
0.0002
0
Drying rate [kgw/kg d.b. min.]
75℃
65℃
55℃
35℃
0
50
100
150
200
250
300
350
400
450
500
550
600
650
700
750
Time [min]

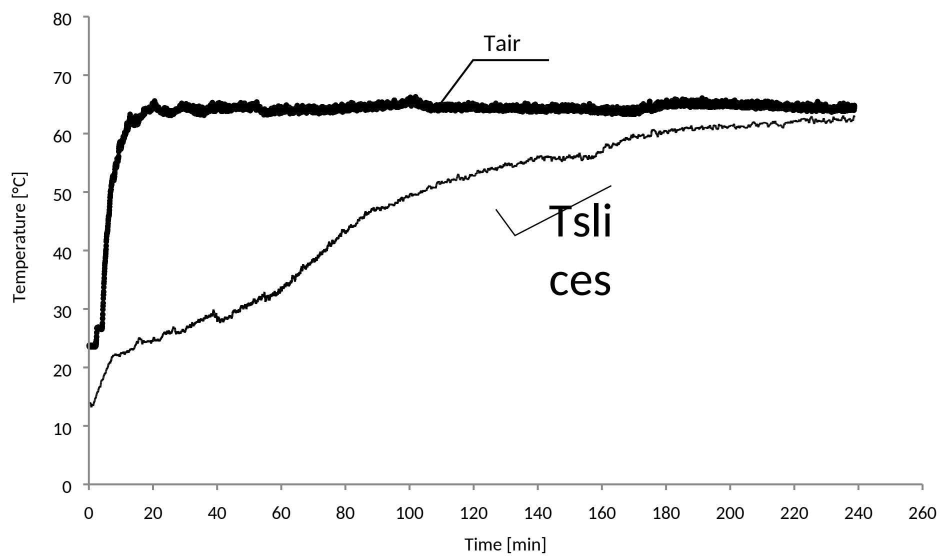

Tair
Tsli
ces
Temperature [ºC]
Time [min]

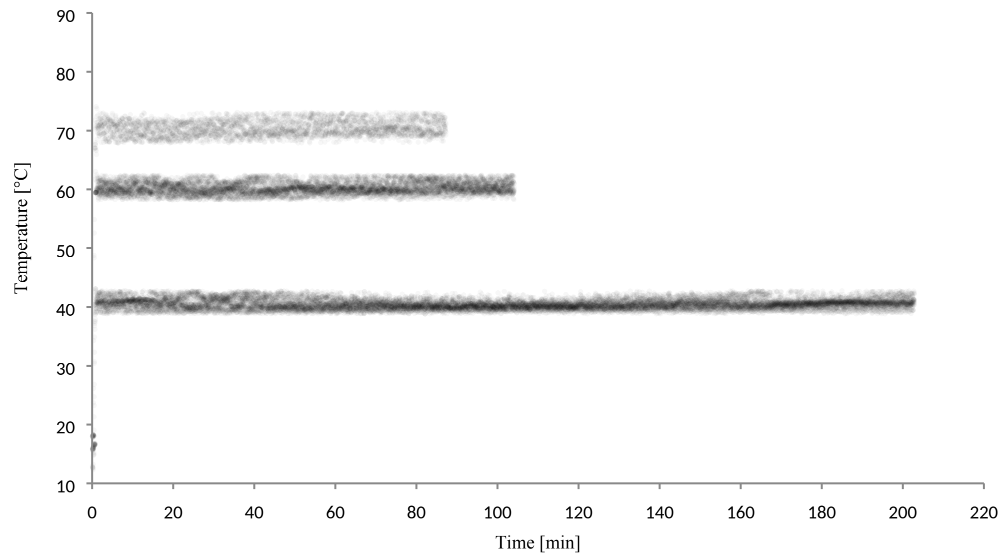
90
80
70
60
50
40
30
20
10
Temperature [°C]
0
20
40
60
80
100
120
140
160
180
200
220
Time [min]

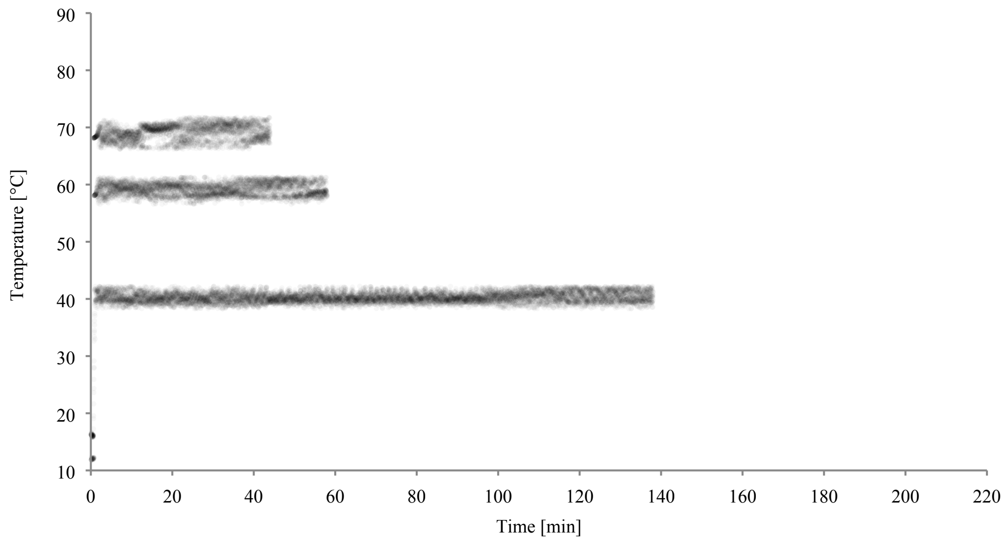

Temperature [°C]
90
80
70
60
50
40
30
20
10
0
20
40
60
80
100
120
140
160
180
200
220
Time [min]

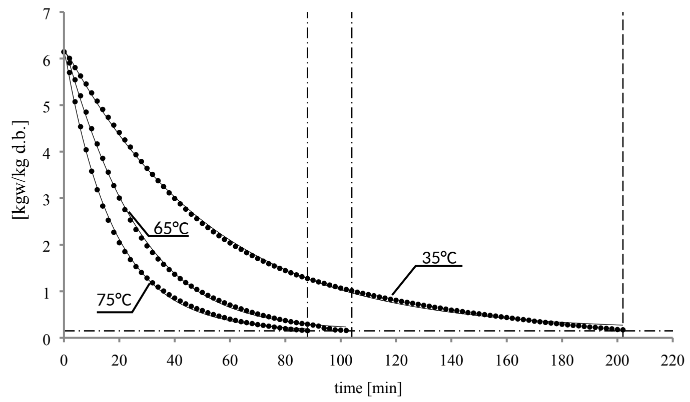

35°C
65°C
75°C
[kgw/kg d.b.]
time [min]

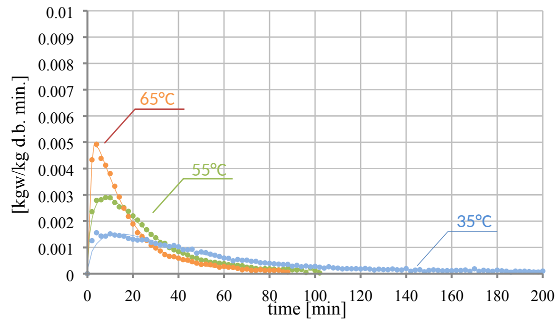
0.01
0.009
0.008
0.007
0.006
0.005
0.004
0.003
0.002
0.001
0
[kgw/kg d.b. min.]
65℃
55℃
35℃
0
20
40
60
80
100
120
140
160
180
200
time [min]

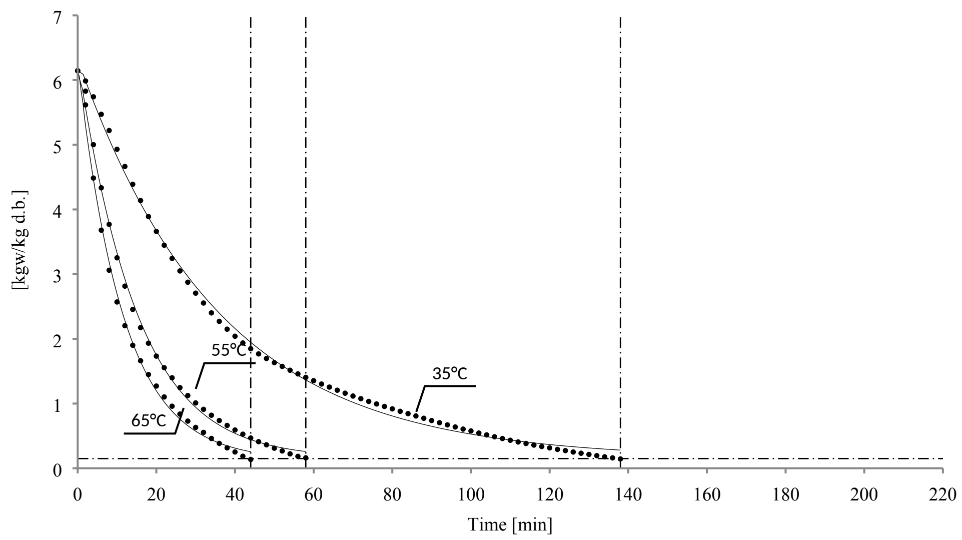

[kgw/kg d.b.]
7
6
5
4
3
2
1
0
55ºC
35ºC
65ºC
0
20
40
60
80
100
120
140
160
180
200
220
Time [min]

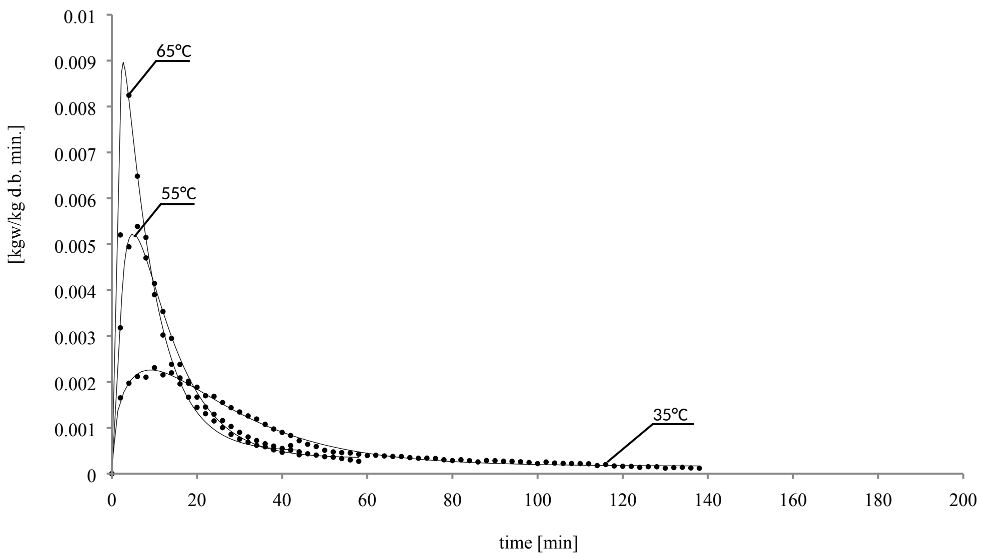

0.01
0.009
0.008
0.007
0.006
0.005
0.004
0.003
0.002
0.001
0
[kgw/kg d.b. min.]
65°C
55°C
35°C
0
20
40
60
80
100
120
140
160
180
200
time [min]

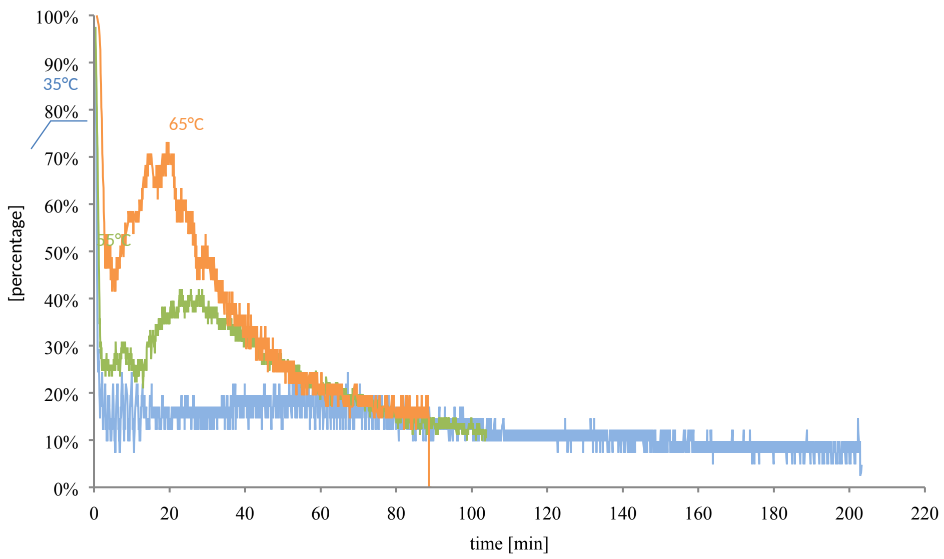
100%
90%
35°C
80%
65°C
70%
60%
50%
40%
30%
20%
10%
0%
[percentage]
0
20
40
60
80
100
120
140
160
180
200
220
time [min]

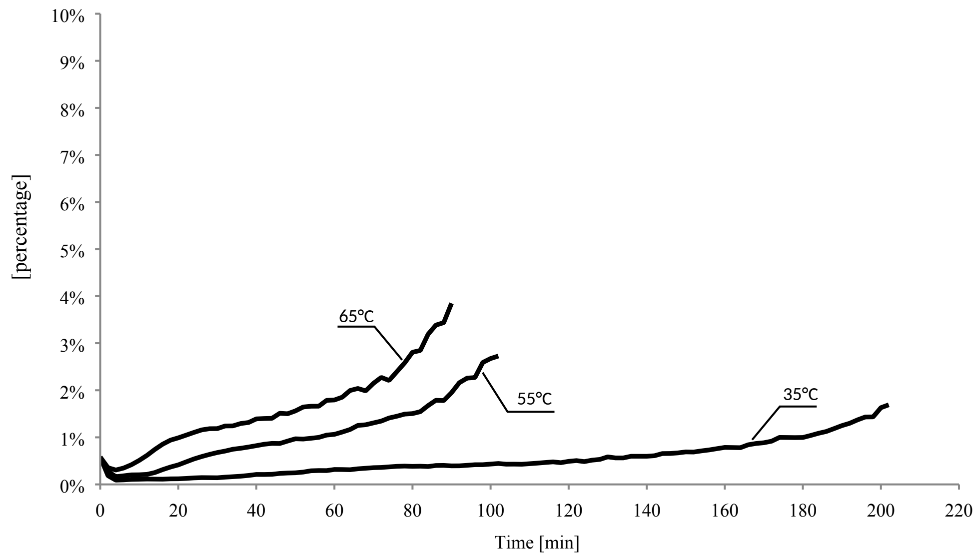

10%
9%
8%
7%
6%
5%
4%
3%
2%
1%
0%
[percentage]
0
20
40
60
80
100
120
140
160
180
200
220
Time [min]
65°C
55°C
35°C

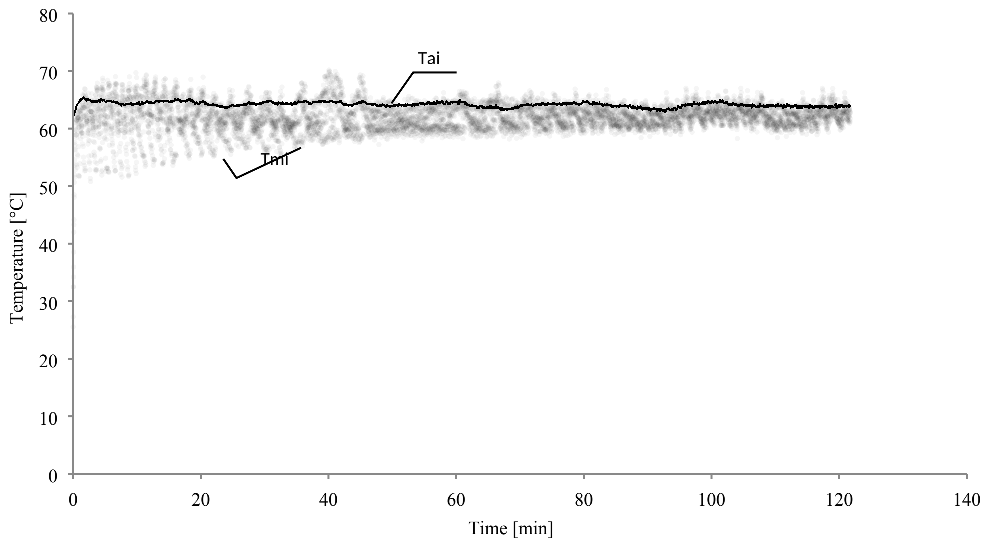

Temperature [°C]
Time [min]
Tai
Tmi
80
70
60
50
40
30
20
10
0
0
20
40
60
80
100
120
140

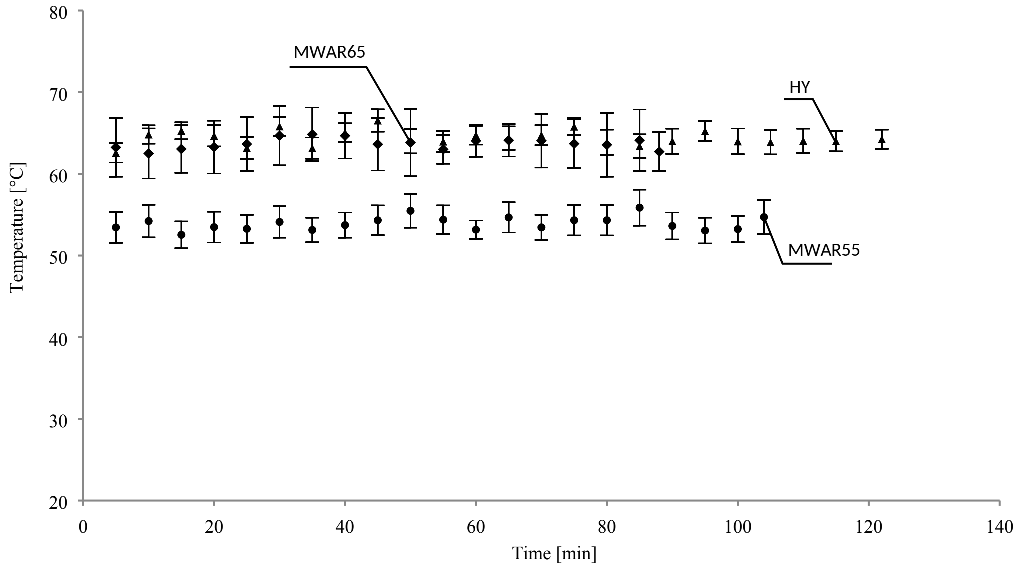
80
70
60
50
40
30
20
Temperature [°C]
0
20
40
60
80
100
120
140
Time [min]
MWAR65
HY
MWAR55

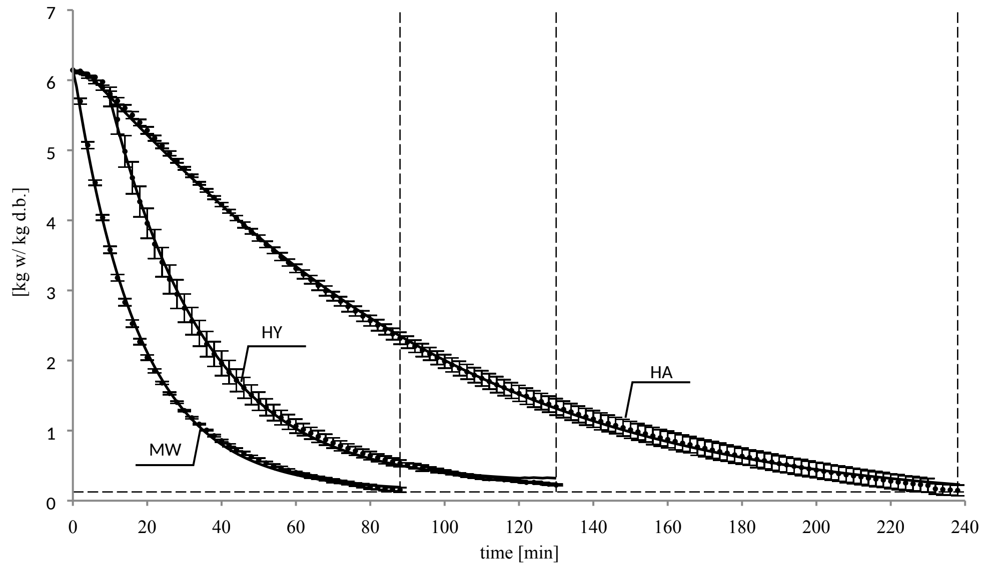

7
6
5
4
3
2
1
0
[kg w/ kg d.b.]
HY
HA
MW
0
20
40
60
80
100
120
140
160
180
200
220
240
time [min]

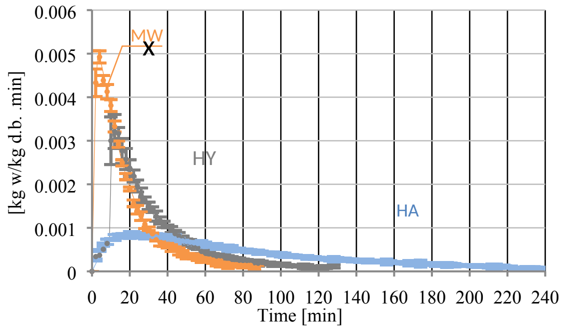

0.006
0.005
0.004
0.003
0.002
0.001
0
[kg w/kg d.b. .min]
MW
X
HY
HA
0 20 40 60 80 100 120 140 160 180 200 220 240
Time [min]

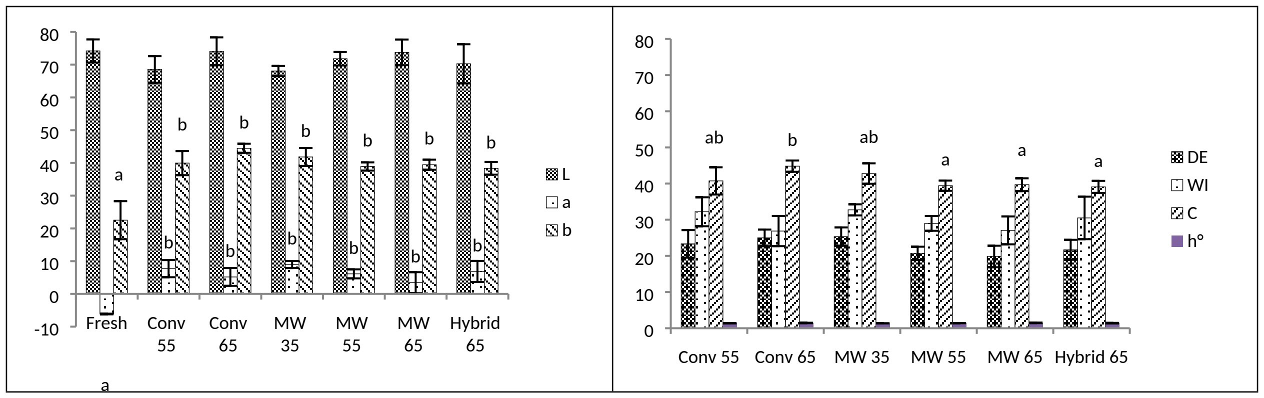
80
70
60
50
40
30
20
10
0
-10
Fresh
Conv 55
Conv 65
MW 35
MW 55
MW 65
Hybrid 65
L
a
b
Conv 55
Conv 65
MW 35
MW 55
MW 65
Hybrid 65
DE
WI
C
h°